Inorg. Chem. **2007**, *46*, 103–107

Inorganic Chemistry

Article

Control of Two-Electron Four-Center ($2e^-$/4c) C–C Bond Formation Observed for Tetracyanoethenide Dimerization, $[TCNE]_2^{2-}$

Juan N. Novoa,*[,†] Jordi Ribas-Ariño,[†] William W. Shum,[‡] and Joel S. Miller*[,‡]

Department of Physical Chemistry, CERQT, and Institute of Nanotechnology and Nanoscience,
University of Barcelona, E-08028 Barcelona, Spain, and Department of Chemistry,
University of Utah, 315 South 1400 East Room 2124, Salt Lake City, Utah 84112-0850

Received June 19, 2006

$Cu(PPh_3)_3(TCNE)$ (TCNE = tetracyanoethylene) and 14 other examples form $[TCNE]_2^{2-}$ dimers possessing a long 2.89 ± 0.05 Å two-electron four-center ($2e^-$/4c) C–C bond in the solid state. This bond arises from the overlap of the b_{2g} π^* singly occupied molecular orbital (SOMO) on each $[TCNE]^{\bullet-}$ fragment, forming a filled bonding orbital of b_{2u} symmetry, and the stabilizing effect of the cation···anion interactions in the crystal that exceed the anionic repulsion. In contrast, $Mn(C_5H_5)(CO)_2(TCNE)$ exhibits a related, but different, $[TCNE]^{\bullet-}\cdots[TCNE]^{\bullet-}$ motif in the solid state that lacks the $2e^-$/4c C–C bonding. To better understand the unusual nature of $2e^-$/4c C–C bonding, the genesis of the differences between their respective π-$[TCNE]^{\bullet-}\cdots[TCNE]^{\bullet-}$ interactions was sought. The lack of $2e^-$/4c C–C bond formation is attributed to the weaker radical character of the $[TCNE]^{\bullet-}$ ligand, which has a total spin population of only 0.5 electron, half of that required for two $S = {}^1/_2$ $[TCNE]^{\bullet-}$ moieties to form a $[TCNE]_2^{2-}$ dimer. Hence, the antiferromagnetic Mn^{II}–$[TCNE]^{\bullet-}$ intramolecular interaction (between the formally $S = {}^1/_2$ Mn-bound $[TCNE]^{\bullet-}$ and the paramagnetic Mn(II)) dominates over the intermolecular π-$[TCNE]^{\bullet-}$–$[TCNE]^{\bullet-}$ spin coupling (between two $S = {}^1/_2$ $[TCNE]^{\bullet-}$ needed to form $[TCNE]_2^{2-}$). Therefore, by selecting specific metal ions that can interact with σ-$[TCNE]^{\bullet-}$, dimerization forming $[TCNE]_2^{2-}$ can be favored or disfavored.

Introduction

Organic compounds exhibiting unusually long C−C bonds have been the focus of several recent studies.[1−5] The longest C−C sp^3−sp^3 single bond reported to date is ∼2.0 Å;[4] however, several eclipsed $[TCNE]_2^{2-}$ (TCNE = tetracyanoethylene) dimers, $\mathbf{1_2}$, form long two-electron π^*−π^* C−C bonds involving four carbon atoms.[3,5] The bond arises from the overlap of the b_{2g} singly occupied molecular orbital (SOMO) $[TCNE]^-$ orbitals to form bonding and antibonding orbitals of b_{2u} and b_{1g} symmetry, respectively, for $[TCNE]_2^{2-}$ (Figure 1) and exhibits the same electronic properties as conventional covalent chemical bonds. These long C−C bonds range from 2.82 to 3.09 Å and average 2.89 Å (Chart 1).[3,5a] The cations range from electrostatically bonded Tl^+ (ref 6) and K^+ (ref 7)to bulky, noncoordinating cations such as $[Cr(C_6H_6)_2]^+$ (ref 8) and $[TDAE]^{2+}$ [TDAE = $(Me_2N)_2CC(NMe_2)_2$].[6]

This bonding motif is also observed for $[Cu^I(PPh_3)_3{}^+](TCNE^{\bullet-})$, **2**.[9] However, $[Mn^{II}(C_5H_5)(CO)_2{}^{\bullet+}](TCNE^{\bullet-})$, **3**, crystallizes with centrosymmetric, but not eclipsed, TCNE···TCNE interactions.[10] The closest intradimer $C_{sp^2}\cdots C_{sp^2}$

---

* To whom correspondence should be addressed. E-mail: jsmiller@chem.utah.edu (J.S.M.), juan.novoa@ub.edu (J.J.N.).

[†] University of Barcelona.

[‡] University of Utah.

(1) Kaupp, G.; Boy, J. *Angew. Chem., Int. Ed. Engl.* **1997**, *36*, 48.

(2) Toda, F. *Eur. J. Org. Chem.* **2000**, *8*, 1377.

(3) (a) Novoa, J. J.; Lafuente, P.; Del Sesto, R. E.; Miller, J. S. *Angew. Chem., Int. Ed.* **2001**, *40*, 2540. (b) Del Sesto, R. E.; Miller, J. S.; Novoa, J. J.; Lafuente, P. *Chem.*—*Eur. J.* **2002**, *8*, 4894. (c) Novoa, J. J.; Lafuente, P.; Del Sesto, R. E.; Miller, J. S. *CrystEngComm* **2002**, *4*, 373.

(4) Teixidor, F.; Viñas, C. *Sci. Synth.* **2005**, *6*, 1235. Brown, D. A.; Clegg, W.; Colquhoun, H. M.; Daniels, J. A.; Stephenson, I. R.; Wade, K. A. *J. Chem. Soc., Chem. Commun.* **1987**, 889. Llop, J.; Viñas, C.; Teixidor, F.; Victori, L.; Kivekäs, R.; Sillanpää, R. *Inorg. Chem.* **2002**, *41*, 3347.

(5) (a) Lu, J.-M.; Rosokha, S. V.; Kochi, J. K. *J. Am. Chem. Soc.* **2003**, *125*, 12161. (b) Jakowski, J.; Simons, J. *J. Am. Chem. Soc.* **2003**, *125*, 16089. (c) Jung, Y.; Head-Gordon, M. *Phys. Chem. Chem. Phys.* **2004**, *6*, 2008.

(6) Johnson, M. T.; Campana, C. F.; Foxman, B. M.; Desmarais, W.; Vela, M. J.; Miller, J. S. *Eur. J. Chem.* **2000**, *6*, 1805.

(7) Bock, H.; Ruppert, K.; Fenske, D.; Goesmann, H. *Z. Anorg. Allg. Chem.* **1995**, *595*, 275.

(8) Miller, J. S.; O'Hare, D. M.; Charkraborty, A.; Epstein, A. J. *J. Am. Chem. Soc.* **1989**, *111*, 7853.

(9) Olmsted, M. M.; Speier, G.; Szabo, L. *J. Chem. Soc., Chem. Commun.* **1994**, 541.

10.1021/ic0611037 CCC: $37.00

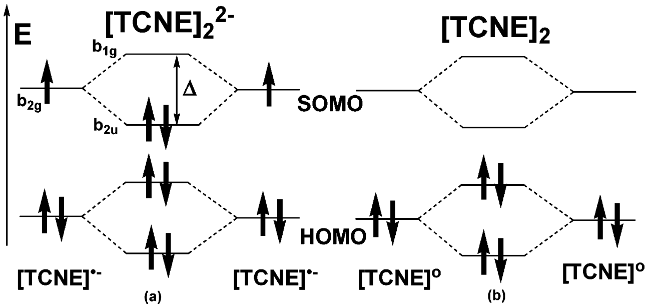

Figure 1. Schematic MO diagram of the b_{2g} SOMO $[TCNE]^{\bullet -}$ orbitals overlapping to form bonding and antibonding orbitals of b_{2u} and b_{1g} symmetry, respectively, for $[TCNE]_2^{2-}$ (a) and $[TCNE]_2$ (b).

separation for $\mathbf{3_2}$ dimers is 3.505 Å (Chart 1), 21% greater than that observed for $\mathbf{2_2}$ dimers. Furthermore, while the three characteristic infrared (IR) υ_{CN} absorptions for the $[TCNE]_2^{2-}$ dimers, including $\mathbf{2_2}$, occur at 2191 ± 2 (m), 2173 ± 3 (s), and 2162 ± 2 (s) cm^{-1},[3a,11] they occur at 2205 and 2136 cm^{-1} for **3**,[10] indicative that $\mathbf{3_2}$ lacks dimers. These υ_{CN} absorptions are also different than those seen in $[TCNE]^n$ ($n = 0$, 2225, 2260 cm^{-1}; $n = 1-$, 2144, 2183 cm^{-1}).[11] Herein, we address the genesis of this difference, which is hypothesized as arising from spin coupling of the $S = {}^1/_2$ $[TCNE]^{\bullet -}$ with the low spin ($S = {}^1/_2$) Mn^{II} in **3**. This attenuates the radical character of the TCNE ligand, as manifested by its reduced spin population, leading to a negligible $\pi^*-\pi^*$ C$-$C bond. This $Mn^{II}-$TCNE interaction differs from the $Cu^{I}-$TCNE interaction found with Cu^{I} in **2**. These results suggest a route to control the formation of π-$[TCNE]_2^{2-}$ dimers in systems where such dimerization is not wanted, as in molecule-based magnets.

Methodological Details

To evaluate the validity of our hypothesis, the electronic properties (localized charges and spin population) on $[TCNE]^{\bullet -}$ in **2** and **3** were calculated via density functional theory (DFT),[12] using the B3LYP nonlocal exchange-correlation functional[13] and the second-order Moller$-$Plesset (MP2) method[14,15] as well as the all-electron split-valence plus polarization basis set[16] at their crystal geometry. Furthermore, diffuse functions on all atoms of TCNE were added to allow for a proper description of the electron density of the anion in case the preferred electron density is such that a net negative charge is present. The diffuse exponents were obtained by multiplying the smallest of all the exponents for the s and p orbitals by 0.1. We confirmed that this provides exponents similar to those usually employed in the literature. To test our results against the use of this basis set, we also carried out calculations using other basis sets and a similar electron distribution, and net atomic charges were found to be similar for the monomers and dimers. We evaluated the triplet state using the unrestricted formulation of the density functional equations. For the singlet, the closed-shell solution was computed using the restricted formulation of these equations, and the broken-symmetry approach was used for the singlet open-shell solution.[17] In a final test of the B3LYP results, we revaluated the energy separation between the singlet closed-shell and open-shell solutions[18] by doing a CASSCF(8,9) calculation[19] (CASSCF(8,9) is a variational multireference MCSCF calculation that uses all the determinants arising from eight electrons placed in nine active orbitals). These CASSCF calculations also confirmed the nature of the broken-symmetry B3LYP singlet wave function and of its electronic distribution.

Results and Discussion

B3LYP calculations on the crystal structure of **2** indicate that the doublet is the ground state. A natural bond orbital (NBO) analysis[20] of the B3LYP wave function was used to obtain the atomic charges. The results of the NBO analysis for **2** indicate that the net charge on $[TCNE]^{\bullet -}$ is -0.90 e^-. Cu has a charge of $+0.80$ e^-, while each PH_3 used as a computational replacement for PPh_3 in **2** has a net positive charge of $+0.10$ e^-. When the same calculations were done on **3**, the ground state was found to be an open-shell singlet, which is 0.6 kcal/mol below the closed-shell singlet state and 16.7 kcal/mol below the triplet state. The CASSCF(8,9) calculations confirmed the order of stability of the three states, with the open-shell state now being 12.2 kcal/mol more stable than the triplet state (in the open-shell singlet ground state, the orbital occupation is 1.94, 1.92, 1.78, 1.95, 0.21, 0.05, 0.01, 0.07, and 0.05 e^-, indicating that the singlet is a mixed closed-shell open-shell[21]). The NBO analysis of the B3LYP wave function for open-shell **3** reveals that the net charge on $[TCNE]^{\bullet -}$ is -0.4 e^-, with Mn, C_5H_5, and CO having charges of 0.5, -0.13, and 0.03 e^-, respectively,

---

(10) Braunwarth, H.; Huttner, G.; Zsolnai, L. *J. Organomet. Chem.* **1989**, *372*, C23.

(11) Miller, J. S. A*ngew. Chem., Int. Ed.* **2006**, *45*, 2508.

(12) Parr, R. G.; Yang, W. *Density Functional Theory of Atoms and Molecules*; Oxford University Press: New York, 1989.

(13) (a) Becke, A. D. *Phys. Rev. A* **1988**, *38*, 3098. (b) Lee, C.; Yang, W.; Parr, R. G. *Phys. Rev. B* **1988**, *37*, 785. (c) Becke, A. D. *J. Chem. Phys.* **1993**, *98*, 5648.

(14) We used the unrestricted formulation of the MP2 method, and the UMP2 method when the state had open-shell orbitals. The theoretical foundations of the MP2 method are properly explained in: Szabo, A.; Olstlund, N. S. *Modern Quantum Chemistry: Introduction to Advanced Electronic Structure Theory*; Macmillan: New York, 1982.

(15) Frisch, M. J.; Trucks, G. W.; Schlegel, H. B.; Scuseria, G. E.; Robb, M. A.; Cheeseman, J. R.; Zakrzewski, V. G.; Montgomery, J. A., Jr.; Stratmann, R. E.; Burant, J. C.; Dapprich, S.; Millam, J. M.; Daniels, A. D.; Kudin, K. N.; Strain, M. C.; Farkas, O.; Tomasi, J.; Barone, V.; Cossi, M.; Cammi, R.; Mennucci, B.; Pomelli, C.; Adamo, C.; Clifford, S.; Ochterski, J.; Petersson, G. A.; Ayala, P. Y.; Cui, Q.; Morokuma, K.; Malick, D. K.; Rabuck, A. D.; Raghavachari, K.; Foresman, J. B.; Cioslowski, J.; Ortiz, J. V.; Stefanov, B. B.; Liu, G.; Liashenko, A.; Piskorz, P.; Komaromi, I.; Gomperts, R.; Martin, R. L.; Fox, D. J.; Keith, T.; Al-Laham, M. A.; Peng, C. Y.; Nanayakkara, A.; Gonzalez, C.; Challacombe, M.; Gill, P. M. W.; Johnson, B. G.; Chen, W.; Wong, M. W.; Andres, J. L.; Head-Gordon, M.; Replogle, E. S.; Pople, J. A. *Gaussian 98*, revision A7; Gaussian, Inc.: Pittsburgh, PA, 1999.

(16) The basis sets used are the SVP basis set of Ahlrichs (Schaefer, A.; Horn, H.; Ahlrichs, R. *J. Chem. Phys.* **1992**, *97*, 2571) for Cu and Mn and the 6-31G(d) basis set for the remaining atoms (Ditchfield, R.; Hehre, W. J.; Pople, J. A. *J. Chem. Phys.* **1971**, *54*, 734).

(17) Noodlemann, L. *J. Chem. Phys.* **1981**, *74*, 5737. Noodlemann, L.; Davidson, E. R. *Chem. Phys.* **1986**, *109*, 131.

(18) The monoreference picture of a closed-shell singlet state is one where all orbitals are doubly occupied, while the associated open-shell state originates from the closed-shell state by exciting one electron from its HOMO to its LUMO. When the HOMO$-$LUMO energy difference in the closed-shell state is small, the open-shell state can be energetically competitive at the Hartree$-$Fock level and with methods that include correlation contributions.

(19) CASSCF is an acronym for Complete Active Self-Consistent Field, a specific form of MCSCF calculations. The characteristics of the CASSCF and MCSCF methods are well described in: Szabo, A.; Olstlund, N. S. *Modern Quantum Chemistry: Introduction to Advanced Electronic Structure Theory*; Macmillan: New York, 1982.

(20) Carpenter, J. E.; Weinhold, F. *THEOCHEM* **1980**, *169*, 41.

Chart 1

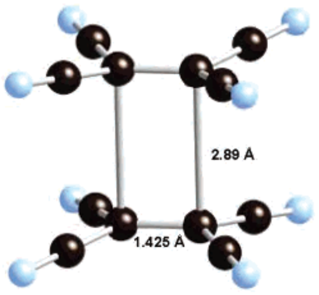

Eclipsed, centrosymmetric $[TCNE]_2^{2-}$, **1**

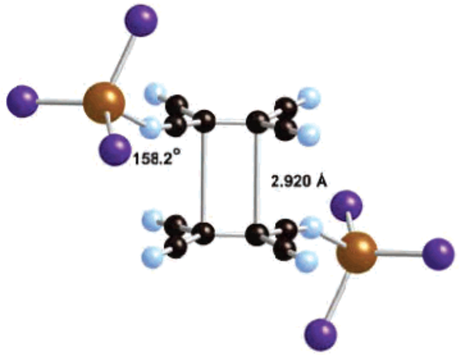

Eclipsed, centrosymmetric $[TCNE]_2^{2-}$ in $Cu^I(PPh_3)_3(TCNE)$, **2** (the Ph rings are not shown for clarity).

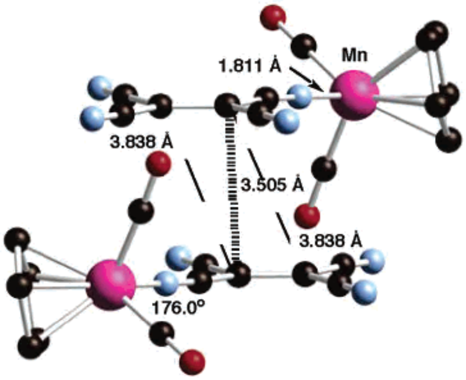

Noneclipsed, centrosymmetric closest $[TCNE]^{\cdot-}\cdots[TCNE]^{\cdot-}$ interactions in $Mn(C_5H_5)(CO)_2(TCNE)$, **3**

with the same results for both the monomer and dimer of **3**. Consequently, although the formal charge of $[TCNE]^{\bullet-}$ in **2** and **3** was originally expected to be the same, our computations reveal that a different degree of charge transfer has occurred for **3**. While $[TCNE]^{\bullet-}$ in **2** has a $-0.9\ e^-$ charge, in **3** it has a $-0.4\ e^-$ charge consistent with the mixed closed-shell open-shell nature of the singlet. The electron distribution difference is observed in the electrostatic potential maps for each molecule (Figure 2). The change in charge distribution also induces a change in the spin localization where one unpaired electron is located in the $[TCNE]^{\bullet-}$ fragment of **2**, but only 0.5 unpaired electrons are located in the $[TCNE]^{\bullet-}$ fragment of **3** (the spin density distributions of **2** and **3** are shown in Figure 3). Thus, an unpaired electron is available on $[TCNE]^{\bullet-}$ in **2** to interact with another nearby $[TCNE]^{\bullet-}$ to form $[TCNE]_2^{2-}$, as seen in other cases.[3] This dimerization is associated with the formation of a $2e^-/4c$ C−C bond that increases the stability of the crystal and is not possible for **3**, as the Cu^I formally does not have any unpaired electrons. Consequently, the $[TCNE]^-\cdots[TCNE]^-$ interaction is different in **2** and **3** (see below).

These differences originate in the different electronic properties associated with the metal−$[TCNE]^{\bullet-}$ interaction in **2** and **3**. In the latter, the bonding orbital is dominated by the metal, thus inducing a partial $[TCNE]^{\bullet-}$-to-metal charge transfer. Furthermore, the interaction between $[TCNE]^{\bullet-}$ and Mn(II) leads to a shorter 1.811 Å Mn−N bond,[10] with respect to the 2.044 Å Cu−N bond observed for Cu(I)−$[TCNE]^{\bullet-}$,[9,22] consistent with the mixed closed-shell open-shell nature of the singlet increasing the Mn−N orbital overlap. The molecular orbital (MO) description of **3** can alternatively be viewed as an antiferromagnetically coupled Mn^{II}−$[TCNE]^{\bullet-}$ ground state, which reduces the radical nature of the $[TCNE]^{\bullet-}$ ligand (due to a ligand-to-metal charge transfer).

It is important to stress that the difference in the net charge of $[TCNE]^-$ in **2** and **3** has important implications with respect to the $[TCNE]^-\cdots[TCNE]^-$ interaction. Two neutral $TCNE^0$ fragments interact via a van der Waals interaction. Its electronic structure (Figure 1) results from the bonding and antibonding combination of the $TCNE^0$ highest occupied molecular orbital (HOMO) and lowest unoccupied molecular orbital (LUMO), with the two orbitals obtained from the HOMO being doubly occupied. This electronic structure is a consequence of the overlap of the monomer orbitals induced by the stabilizing interaction of the two $TCNE^0$ fragments present. This interaction is dominated by its

---

(21) In a monoreference closed-shell singlet configuration, all orbitals should have occupations of 2, while the empty orbitals should have an occupation of 0. In a monoreference open-shell singlet, the doubly occupied orbitals should have occupations of 2, the singly occupied orbitals should have an an occupation of 1, and the empty orbitals should have an occupation of 0. The observed fractional occupancies originate when the singlet wave function has a multireference character, with varying participation of the closed-shell and open-shell configurations.

(22) This difference is not due to crystal effects, as a full geometry optimization of the isolated monomer gives similar changes in the metal−N bond.

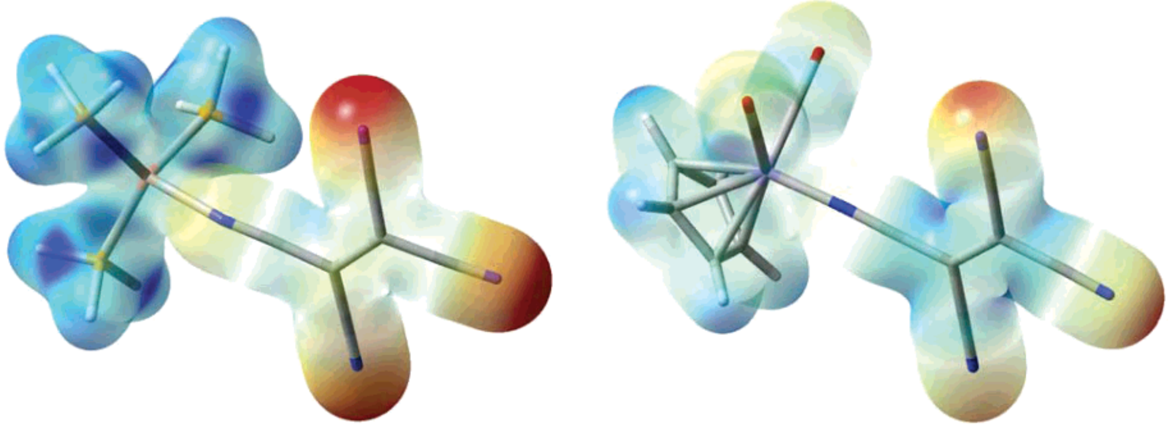

Figure 2. Charge distribution for compounds **2** and **3**, mapped on the isodensity surface of 0.02 atomic units. Red represents negative charge, while blue represents positive charge.

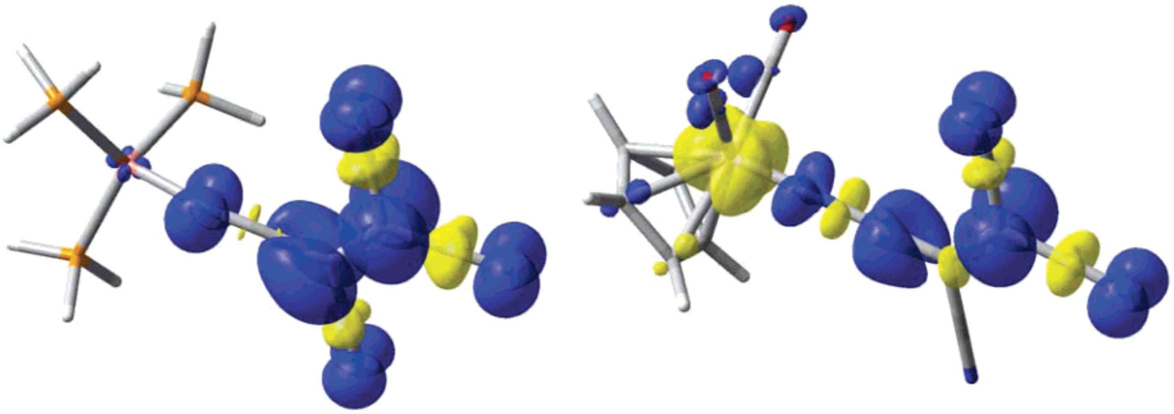

Figure 3. Spin density distribution for **2** and **3** (isosurface of 0.002 atomic units (e$^-$/bohr^3). Blue represents positive spin density regions, while yellow represents negative spin density regions. For consistency, the central TCNE C's have a positive spin for both **2** and **3**, and this is opposite to that which is reported in Table 1 for **3**.

Table 1. Spin and Charge Densities for **2** (Doublet) and **3** (Open-Shell Singlet)

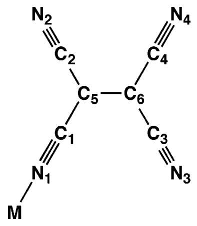

	spin density		charge density	
	2	**3**	**2**	**3**
M = Cu/Mn	0.00	0.62	0.76	0.50
C(1)	0.00	−0.07	0.43	0.38
C(2)	−0.05	0.00	0.28	0.27
C(3)	−0.08	0.07	0.28	0.26
C(4)	−0.09	0.08	0.27	0.26
C(5)	0.22	0.02	−0.33	−0.22
C(6)	0.43	−0.31	−0.27	−0.20
N(1)	0.13	−0.03	−0.60	−0.39
N(2)	0.11	−0.01	−0.33	−0.25
N(3)	0.16	−0.12	−0.34	−0.26
N(4)	0.17	−0.14	−0.32	−0.25
total/TCNE	1.00	−0.51	−0.93	−0.40

dispersion component, a nonclassical term that can be associated with the instantaneous interactions between the electrons in each fragment. The interaction between two [TCNE]$^-$ fragments is distinctly different. Here, in addition to this overlap, the extra electron residing in the two b$_{2g}$ SOMOs (formally the LUMO in TCNE^0) provides two electrons for the b$_{2u}$ dimer bonding combination (Figure 1). This is the type of diagram expected for classical bond formation with the main differences being (a) the SOMOs being combined in [TCNE]$^-$ are antibonding orbitals (π*) and (b) the [TCNE]$^-$···[TCNE]$^-$ dimer is energetically unstable due to the net charge of each monomer. Therefore, the overlap of the SOMOs of **2** (mostly located on each [TCNE]$^-$ fragment) that forms the **2**$_2$ dimer[23] is, in part, a consequence of the attractive cation−anion interactions that exceed the repulsive anion−anion interactions involving the different formal parts of the **2**$_2$ dimer.[5] Based upon the net charge computed at the B3LYP level, the [TCNE]^n···[TCNE]^n interaction in **2** is a 2e$^-$/4c C−C bond, while for **3**, having only one electron in the π* orbital, it might be considered between a 2e$^-$/4c C−C bond and a van der Waals interaction.

The results of the MP2 calculations[15] for **2**$_2$ and **3**$_2$ are consistent with the above description. The MP2 interaction energy as a function of the C−C distance was computed for isolated [TCNE]$_2^n$ (n = 0, 2−) dimers (Figure 4) and the **2** and **3** dimers using the same basis set employed above.[24] In

---

(23) In **2**$_2$, these interactions originate in the charges associated with the formal parts of the two **2** monomers of the [TCNE]$^{0.9-}$ and Cu(PH$_3$)$_3^{0.9+}$ fragments.

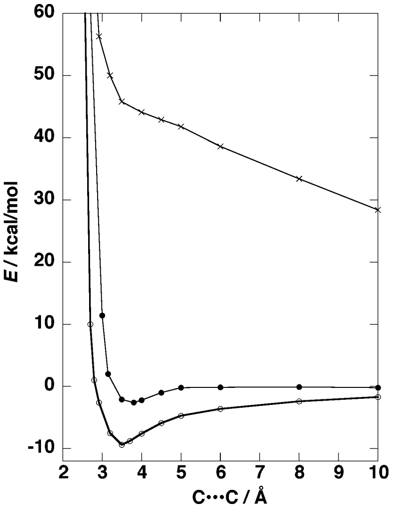

Figure 4. Interaction energies of two neutral TCNE fragments (●), two $[TCNE]^{\bullet-}$ anions (×), and two compound **2** complexes (○), where the intradimer C−C distance is changed, preserving the orientation of the dimers and in the crystal (see text). The same two C atoms were used as reference in all cases.

all cases, the relative orientation of the two interacting fragments was preserved as in the crystal. The results clearly show the different energetic nature of the $[TCNE]^n\cdots[TCNE]^n$ ($n = 0$, $1-$) interactions. The $n = 0$ dimer is stable by ~2.6 kcal/mol (12.5 kJ/mol), while the $n = 1-$ dimer is always repulsive, with a value of 56 kcal/mol (270 kJ/mol) when the C−C distance is 2.920 Å between the $[TCNE]_2^{2-}$ dimers in the crystal of **2**. However, despite the −0.9 e^- net charge on the $[TCNE]^-$ fragment in **2**, the UMP2 interaction energy curve for the $\mathbf{2_2}$ dimers has a minimum at ~3.50 Å, and its energy at the crystal geometry is −2.6 kcal/mol. This is a confirmation that the $[TCNE]^{0.9-}\cdots Cu(PH_3)_3{}^{0.9+}$ interaction is capable of overcompensating the $[TCNE]^{0.9-}\cdots[TCNE]^{0.9-}$ repulsion.

While the magnetic moment for isolated (monomeric) **3** has not been reported, the room-temperature moment is 1.1 μ_B/Mn in the solid state.[10] This paramagnetic behavior is attributed to the thermal population of the triplet state of monomeric **3**. It can also be attributed to the thermal population of the $\mathbf{3_2}$ dimer triplet state. B3LYP calculations on **3** and the crystal structure of $\mathbf{3_2}$, using the same basis set employed in all previous calculations, indicate that the singlet−triplet energy separations in **3** and $\mathbf{3_2}$ are 15.2 and 11.8 kcal/mol, respectively. These values are indicative of the magnitude of the energy separation and suggest that the population of the excited state of $\mathbf{3_2}$ may be the source of the reported room-temperature magnetic moment.

The genesis of the difference of $[TCNE]_2^{2-}$ dimer formation for $Cu(PPh_3)_3(TCNE)$, but not for $Mn(C_5H_5)(CO)_2$-(TCNE), is attributed to the $M-[TCNE]^{\bullet-}$ for the latter having stronger spin coupling than $[TCNE]^{\bullet-}\cdots[TCNE]^{\bullet-}$. Hence, the proper selection of the metal ion and its oxidation state for a $M-[TCNE]^{\bullet-}$ fragment can delocalize the $[TCNE]^{\bullet-}$ unpaired electron spin onto the metal. This delocalization has important effects on the ability of the $[TCNE]^{\bullet-}$ to spin couple via weakening the $[TCNE]^{\bullet-}\cdots[TCNE]^{\bullet-}$ interactions to form $[TCNE]_2^{2-}$ dimers. This is useful for the design of new $[TCNE^-]$-based, molecule-based magnets where such dimerization is avoided, or π-dimers with $2e^-/4c$ bonds.

Acknowledgment. J.S.M. and W.W.S. gratefully acknowledge helpful discussions with Jack Simons (Utah), the support from the NSF (Grant No. CHE0110685) and the DOE (Grant No. DE FG 03-93ER45504), and computer allocation provided by the Center for High Performance Computing at the University of Utah. J.N.N. and J.R. acknowledge the Spanish "Ministerio de Ciencia y Ciencia" and the Catalan CIRIT for grants (# BQU2002-04587-C02-02 and 2001SGR-0044, respectively) and the CEPBA-IBM Research Institute, CEPBA, and CESCA for the allocation of CPU time on their computers. J.R. also acknowledges a "Ministerio de Ciencia y Ciencia" Ph.D. grant.

IC0611037

---

(24) A full-geometry optimization of these dimers was not performed as it is well-known that, when optimized, the results have no similarity with those observed as the structure is a compromise between all interactions made with their nearby molecules.